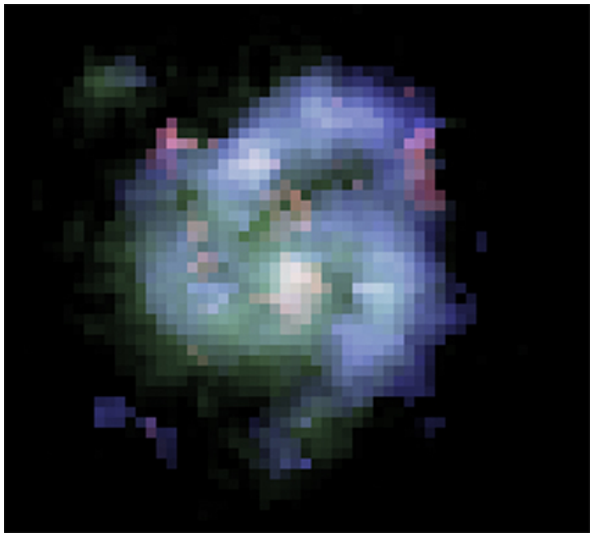

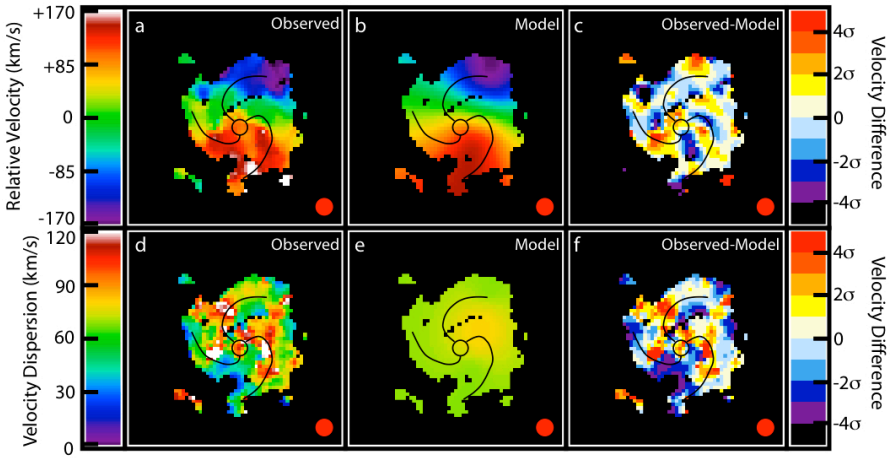

D. R. Law et al 2012, Nature
“Grand Design Spiral at z=2.17”

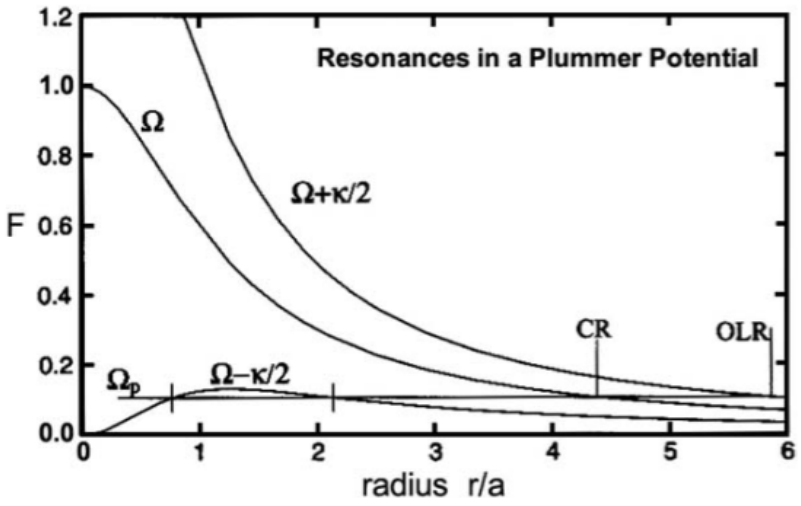

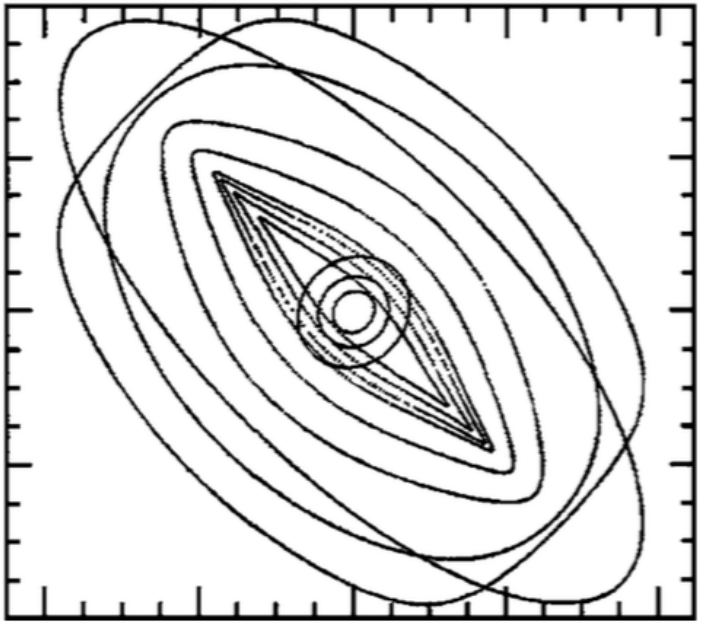

Figure 4 (*Top*) Frequencies $\Omega(r) = V(r)/r$ and $\Omega \pm \kappa/2$, where $\kappa^2 = (2V/r)(V/r + dV/dr)$ is the epicyclic frequency of radial oscillations for almost circular orbits. This figure (Sparke & Gallagher 2000) is for a Plummer potential, but the behavior is generic. For a pattern speed Ω_p, the most important resonances occur where $\Omega_p = \Omega$ (corotation), $\Omega_p = \Omega + \kappa/2$ [outer Lindblad resonance (OLR)], and $\Omega_p = \Omega - \kappa/2$ [two inner Lindblad resonances (ILR), marked with vertical dashes]. (*Bottom*) From Englmaier & Gerhard (1997), examples of the principal orbit families for a bar oriented at 45° as in Figure 7. The elongated orbits parallel to the bar are the x_1 family out of which the bar is constructed. Interior to ILR (or outer ILR, if there are two LRs), the x_2 family is perpendicular to the bar. Near corotation is the 4:1 ultraharmonic resonance; the almost-square orbit makes four radial oscillations during each circuit around the center. Since the principal orbits change orientation by 90° at each resonance shown, they must cross near the resonances.

Kormendy & Kenicutt ARAA 2004

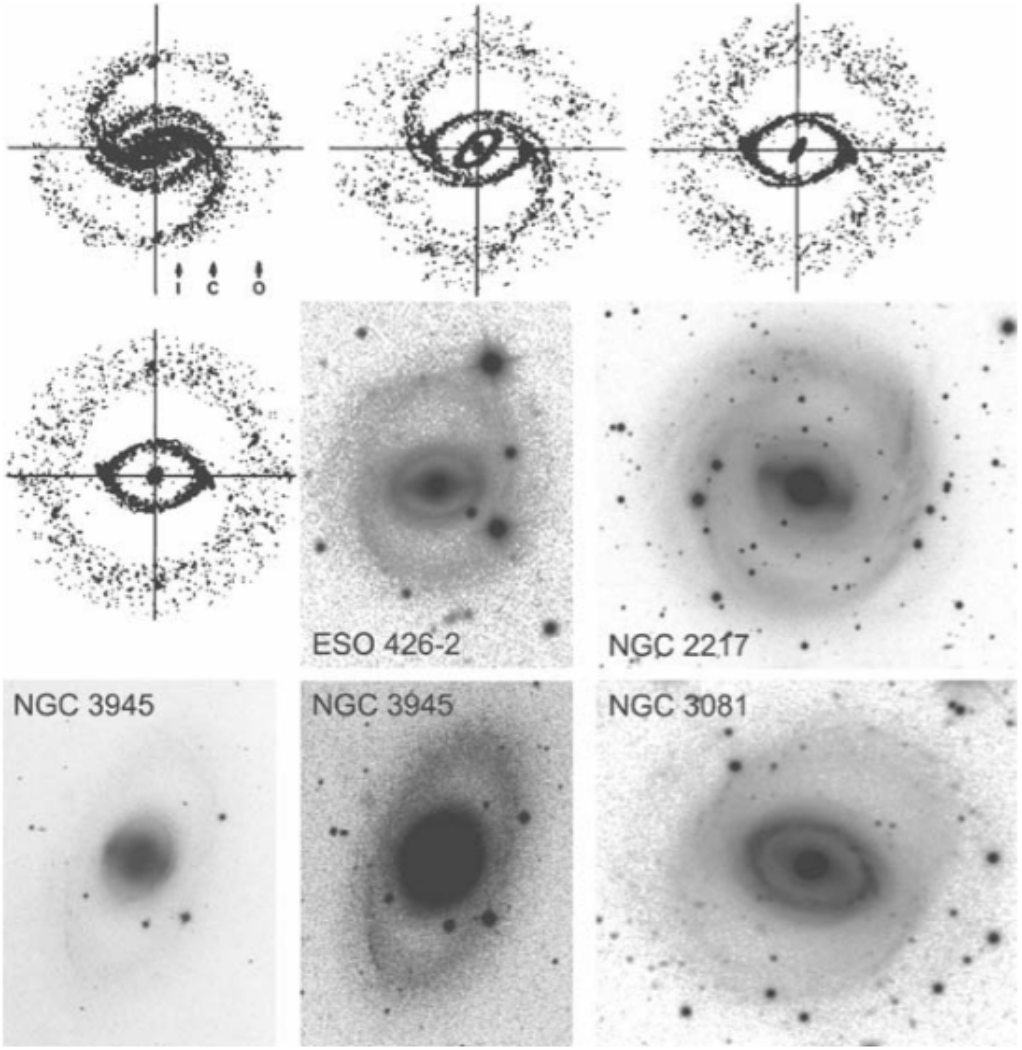

Figure 5 Evolution of gas in a rotating oval potential (Simkin, Su, & Schwarz 1980; see also Schwarz 1981, 1984). The gas particles in this sticky-particle *n*-body model are shown after 2, 3, 5, and 7 bar rotations (*top-left through center-left*). Arrows show the radii of ILR, corotation, and OLR. Four SB0 or SB0/a galaxies are shown that have outer rings and a lens (NGC 3945) or an inner ring (obvious in ESO 426-2 and in NGC 3081, but poorly developed in NGC 2217). Sources: NGC 3945 (Kormendy 1979b); NGC 2217, NGC 3081 (Buta et al. 2003); ESO 426-2 (Buta & Crocker 1991).

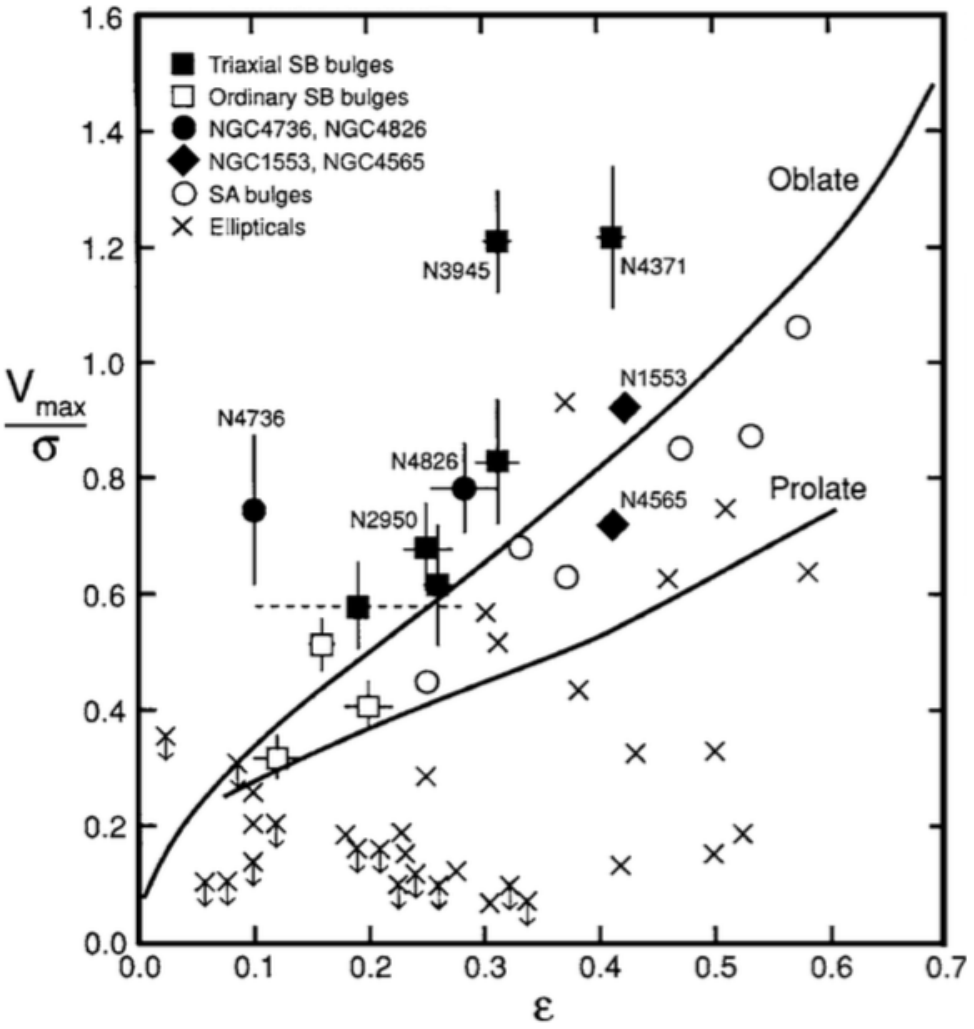

Figure 17 The relative dynamical importance of rotation and random motions as a function of observed ellipticity for various kinds of stellar systems. Here V_{max}/σ is the ratio of maximum rotation velocity to mean velocity dispersion interior to the half-light radius and $\epsilon = 1 -$ axial ratio. The "oblate" line describes oblate-spheroidal systems that have isotropic velocity dispersions and that are flattened only by rotation; it is a consequence of the tensor virial theorem (Binney & Tremaine 1987). The "prolate" line is one example of how prolate spheroids can rotate more slowly for a given ϵ because they are flattened partly by velocity dispersion anisotropy. This figure is updated from Kormendy (1993).

Interacting Galaxies

Hubble Space Telescope • ACS/WFC • WFPC2

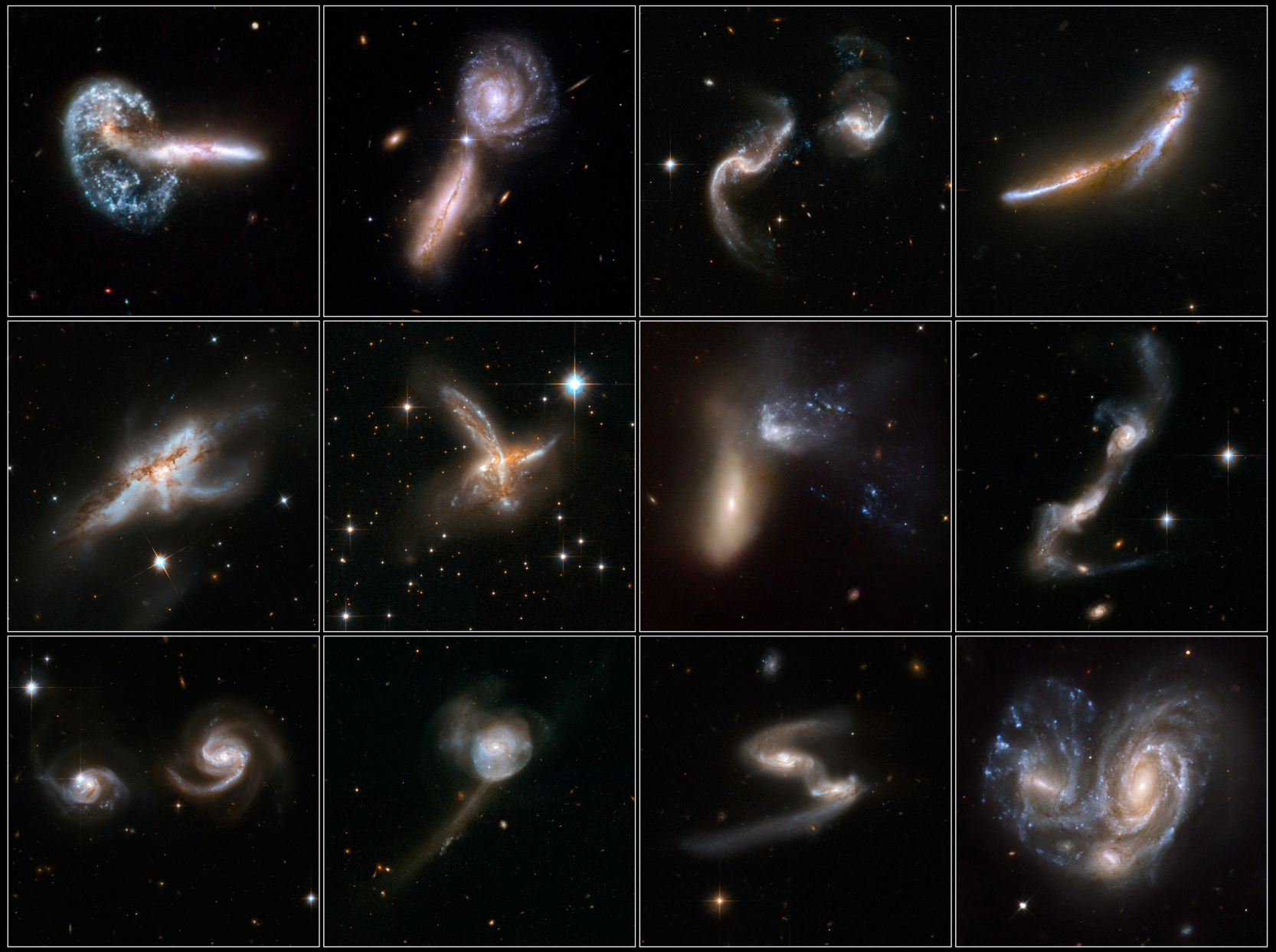

NASA, ESA, the Hubble Heritage (AURA/STScI)-ESA/Hubble Collaboration, and
A. Evans (University of Virginia, Charlottesville/NRAO/Stony Brook University)

STScI-PRC08-16a

The “Antennae”

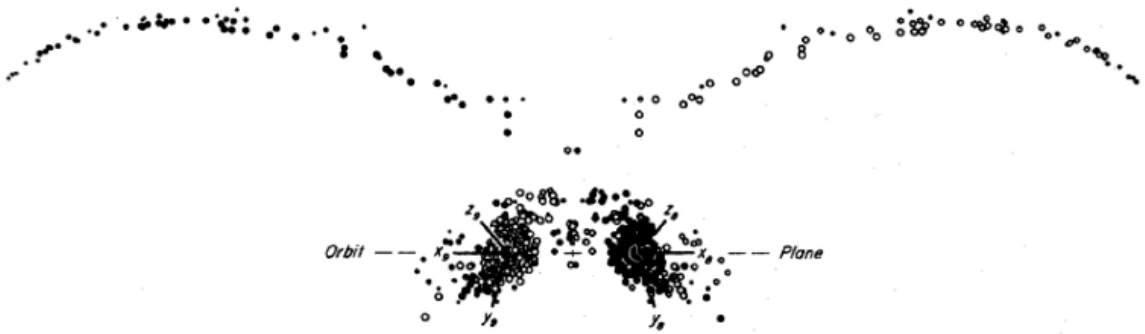

FIG. 23.—Symmetric model of NGC 4038/9. Here two identical disks of radius $0.75R_{\min}$ suffered an $e \approx 0.5$ encounter with orbit angles $i_8 = i_9 = 60°$ and $\omega_8 = \omega_9 = -30°$ that appeared the same to both. The above all-inclusive views of the debris and remnants of these disks have been drawn exactly normal and edge-on to the orbit plane; the latter viewing direction is itself 30° from the line connecting the two pericenters. The viewing time is $t = 15$, or slightly past apocenter. The filled and open symbols again disclose the original loyalties of the various test particles.

Toomre & Toomre 1972, ApJ 178, 623

Sbc Galaxy: Major Merger

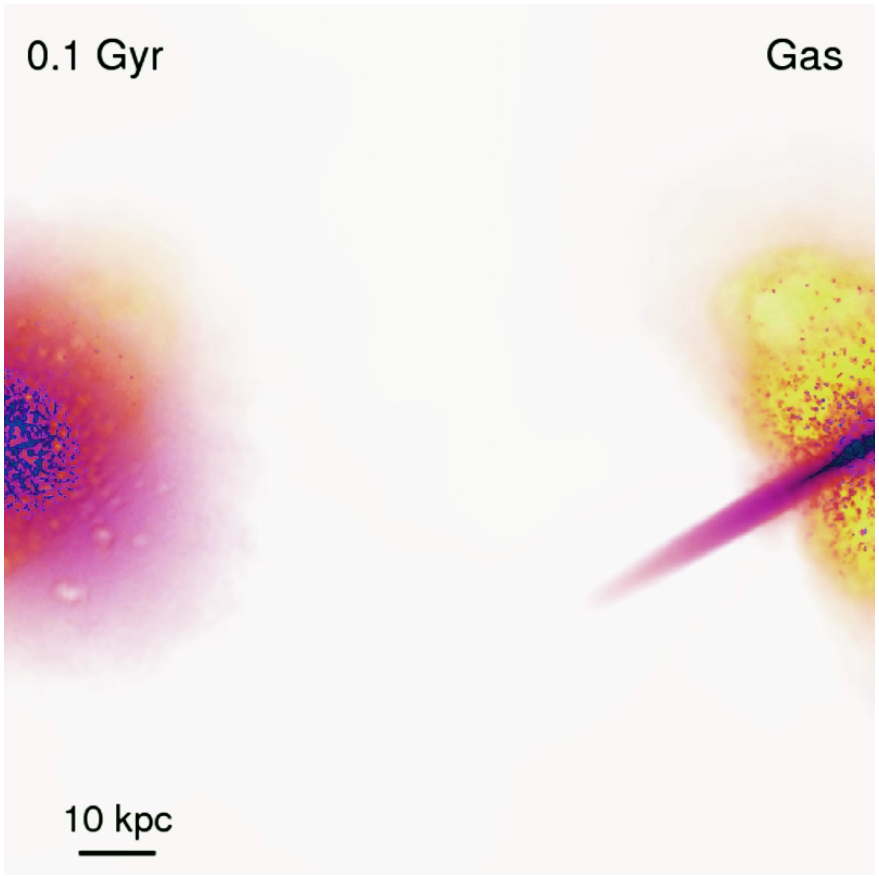

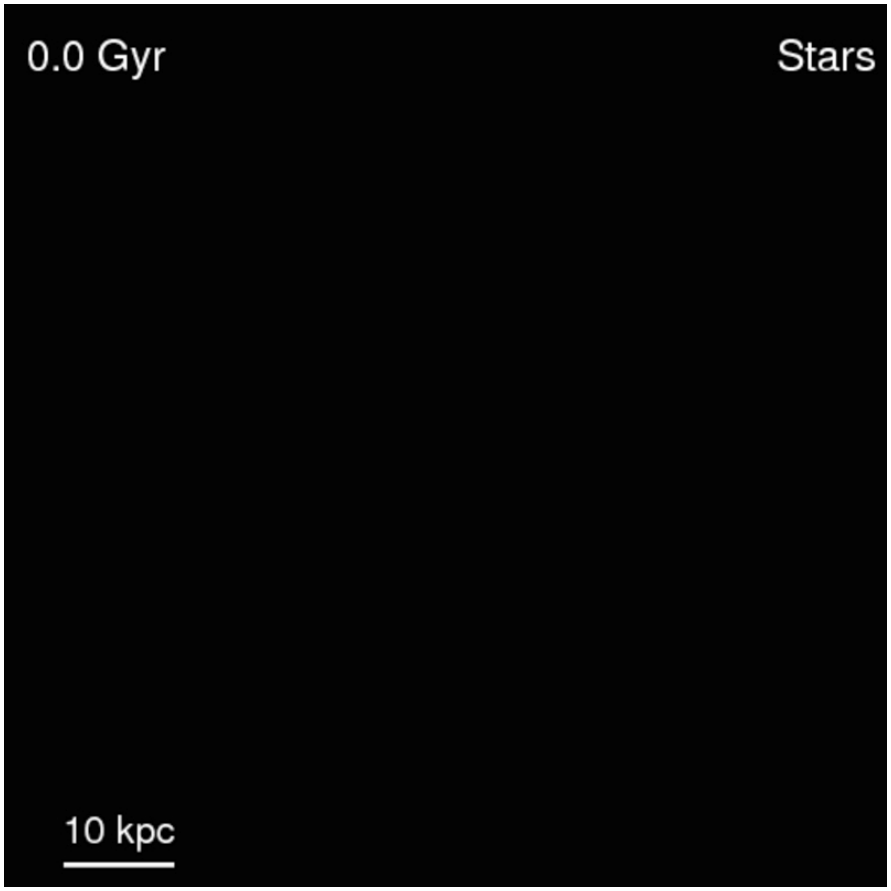

Credit: P. Hopkins et al
(www.tapir.caltech.edu/~phopkins)

High Redshift Major Merger

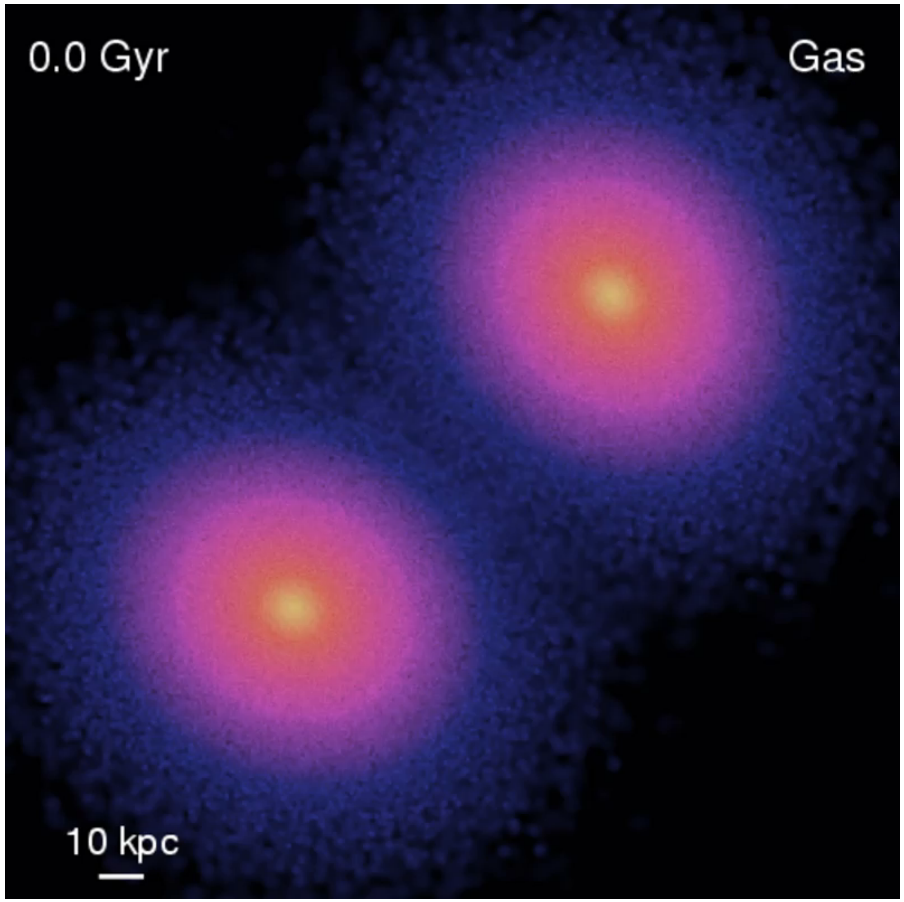

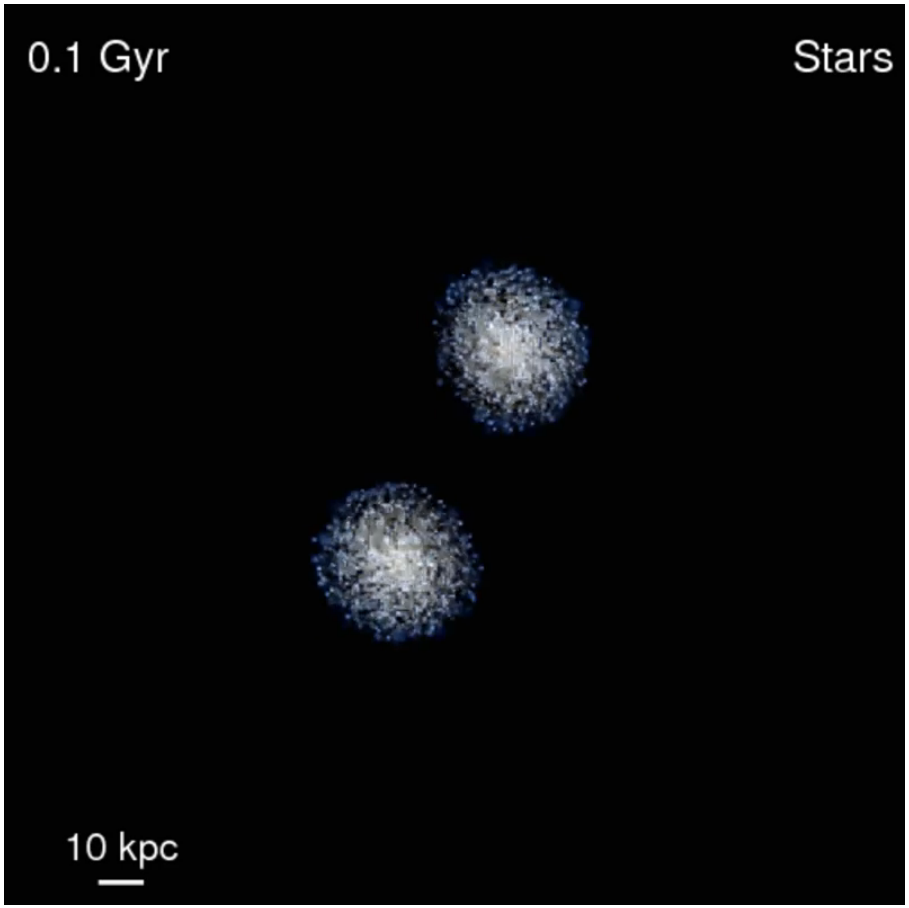

Credit: P. Hopkins et al
(www.tapir.caltech.edu/~phopkins)